Spin-orbit torques in strained PtMnSb from first principles

Frank Freimuth [1,2,*] Stefan Blügel [1] and Yuriy Mokrousov [1,2]

[1] *Peter Grünberg Institut and Institute for Advanced Simulation, Forschungszentrum Jülich and JARA, 52425 Jülich, Germany*

[2] *Institute of Physics, Johannes Gutenberg University Mainz, 55099 Mainz, Germany*

(Received 26 March 2021; revised 31 May 2021; accepted 2 June 2021; published 11 June 2021)

We compute spin-orbit torques (SOTs) in strained PtMnSb from first principles. We consider both tetragonal strain and shear strain. We find a strong linear dependence of the field-like SOTs on these strains, while the antidamping SOT is only moderately sensitive to shear strain and even insensitive to tetragonal strain. We also study the dependence of the SOT on the magnetization direction. In order to obtain analytical expressions suitable for fitting our numerical *ab initio* results we derive a general expansion of the SOT in terms of all response tensors that are allowed by crystal symmetry. Our expansion includes also higher-order terms beyond the usually considered lowest order. We find that the dependence on the strain is much smaller for the higher-order terms than for the lowest order terms. In order to judge the sensitivity of the SOT to the exchange correlation potential we compute the SOT in both GGA and LDA. We find that the higher-order terms depend significantly on the exchange-correlation potential, while the lowest order terms are insensitive to it. Since the higher-order terms are small in comparison to the lowest order terms the total SOT is insensitive to the exchange correlation potential in strained PtMnSb.

DOI: 10.1103/PhysRevB.103.224414

I. INTRODUCTION

The spin-orbit torque (SOT) allows us to switch the magnetization by electric current in noncentrosymmetric bulk crystals and in bilayers with structural inversion asymmetry [1]. It therefore paves the way to novel spintronic memory devices. Among the noncentrosymmetric bulk crystals the half-metallic half-Heusler compounds are promising for spintronics applications [2–5]. In particular, their high conduction-electron spin-polarization enhances for example the tunneling magnetoresistance and the giant magnetoresistance [6–9], and their half-metallicity suppresses the Gilbert damping [10].

The SOT in the half-Heusler NiMnSb depends strongly on the strain, which may be controlled by varying the substrate [11,12]. Notably, NiMnSb thin films sputtered on GaAs substrates yield SOT effective fields per applied current that are similar in magnitude to those in $Pt/Co/AlO_x$ magnetic bilayers [13]. Tetragonal strain adds Dresselhaus spin-orbit interaction (SOI) to the microscopic half-Heusler Hamiltonian, while shear strain supplements it with both Rashba and Dresselhaus SOI.

The SOTs arising from Dresselhaus and Rashba SOI correspond to the lowest order in the expansion of the SOT with respect to the magnetization [14]. In magnetic bilayers the higher-order terms in this expansion have been found to be sizeable in experiments [15], and several theoretical works have therefore considered the dependence of the SOT on the magnetization direction in detail in these bilayer systems [16–18]. However, in the case of half-Heusler crystals the higher-order contributions in the expansion of the SOT in terms of the directional cosines of the magnetization have not yet been considered. Therefore, our symmetry analysis of the SOT in this paper includes also the first higher-order terms in the directional cosine expansion. Such angular expansions may be used to fit experimental SOT data [15]. In the present paper we use the angular expansion in order to fit our *ab initio* data, which allows us to separate the SOT into the lowest-order Dresselhaus and Rashba SOI contributions and the remaining higher-order terms.

PtMnSb is a promising material for spintronics applications. Its half-metallicity has been established both experimentally and theoretically. It can be grown epitaxially on MgO(001) [19] and on W(001)/MgO(001) [20]. It exhibits a giant magneto-optical Kerr effect [21,22], which makes it attractive for magneto-optical recording. Furthermore, it exhibits a negative anisotropic magnetoresistance and it has been used for room-temperature giant magnetoresistance devices [23,24]. In this paper we discuss the SOT in PtMnSb with tetragonal and shear strain obtained from first-principles density-functional theory calculations.

This paper is structured as follows: In Sec. II we discuss the form of the SOT expected in half Heuslers based on the symmetry of the cubic, tetragonally strained, and shear-strained crystals. The tetragonally strained case is discussed in detail in Sec. II, while the cubic and the shear-strained cases are discussed in detail in the Appendices A and B. In Sec. III we present our *ab initio* results on the SOTs in PtMnSb. In Sec. III A we describe the computational details. In Sec. III B we discuss the results on the odd torque and in Sec. III C we discuss the results on the even torque. This paper ends with a summary in Sec. IV.

II. SYMMETRY OF SOTS IN HALF-HEUSLER CRYSTALS

Similar to the conductivity tensor, which measures the response of the electric current to an applied electric field in

*Corresponding author: f.freimuth@fz-juelich.de

linear response, we introduce the torkance tensor to quantify the response of the torque to an applied electric field [25]. The torque $\boldsymbol{T}$ acting on the magnetization in one crystal unit cell is written as

$$\boldsymbol{T} = \sum_{ij} \hat{\boldsymbol{e}}_i t_{ij} E_j, \tag{1}$$

where t_{ij} is the torkance tensor, E_j is the j-th component of the applied electric field, and $\hat{\boldsymbol{e}}_i$ is a unit vector in the i-th Cartesian direction. In cubic and tetragonally strained PtMnSb the crystal lattice vectors $\boldsymbol{a}$, $\boldsymbol{b}$, and $\boldsymbol{c}$ used in the following sections are related to $\hat{\boldsymbol{e}}_i$ by $\boldsymbol{a} = a\hat{\boldsymbol{e}}_1$, $\boldsymbol{b} = b\hat{\boldsymbol{e}}_2$, and $\boldsymbol{c} = c\hat{\boldsymbol{e}}_3$, where a, b, and c are the lattice constants. In shear-strained PtMnSb we choose the $\boldsymbol{a}$ and $\boldsymbol{b}$ axes as follows:

$$\boldsymbol{a} = a\left(\cos\frac{\epsilon}{2}, \sin\frac{\epsilon}{2}, 0\right)^{\mathrm{T}}, \quad \boldsymbol{b} = a\left(\sin\frac{\epsilon}{2}, \cos\frac{\epsilon}{2}, 0\right)^{\mathrm{T}}, \tag{2}$$

where we use $\epsilon = 90^\circ - \gamma$ to quantify the shear strain, and γ is the angle between the $\boldsymbol{a}$ and $\boldsymbol{b}$ axes.

We separate the torkance into even and odd parts with respect to inversion of the magnetization direction, i.e., $\boldsymbol{t}(\hat{\boldsymbol{M}}) = \boldsymbol{t}^{\mathrm{even}}(\hat{\boldsymbol{M}}) + \boldsymbol{t}^{\mathrm{odd}}(\hat{\boldsymbol{M}})$, where $\boldsymbol{t}^{\mathrm{even}}(\hat{\boldsymbol{M}}) = [\boldsymbol{t}(\hat{\boldsymbol{M}}) + \boldsymbol{t}(-\hat{\boldsymbol{M}})]/2$ and $\boldsymbol{t}^{\mathrm{odd}}(\hat{\boldsymbol{M}}) = [\boldsymbol{t}(\hat{\boldsymbol{M}}) - \boldsymbol{t}(-\hat{\boldsymbol{M}})]/2$. The corresponding even SOT is often referred to as the antidamping SOT, while the odd SOT is often referred to as the field-ike SOT. t_{ij} is an axial tensor of rank 2. It is possible to use the symmetries of the half-Heusler crystal in order to determine the form of t_{ij}. In practice only the torque perpendicular to the magnetization is of relevance and our *ab initio* approach described in Sec. III A computes only this perpendicular component by construction. However, in general, an axial tensor of rank 2 consistent with the crystal symmetry may predict also a component of the torque that is parallel to the magnetization. In order to avoid this irrelevant component we consider instead the symmetry of the effective magnetic field $\boldsymbol{B}$ that one would have to apply in order to generate a torque of the same size as the SOT. After determining the symmetry-allowed form of the response of $\boldsymbol{B}$ to an applied electric field we may subsequently obtain the torque from $\boldsymbol{T} = \mu\hat{\boldsymbol{M}} \times \boldsymbol{B}$. Here, μ is the magnetic moment within one unit cell and $\hat{\boldsymbol{M}}$ is its direction. This approach guarantees that the torque $\boldsymbol{T}$ is perpendicular to the magnetization such that it is not necessary to remove irrelevant contributions obtained from symmetry analysis.

A. Odd torque

The effective field of the odd torque can be expressed in terms of the electric field $\boldsymbol{E}$ and the magnetization direction $\hat{\boldsymbol{M}}$ as follows:

$$B_i^{\mathrm{odd}} = \chi_{ij}^{(\mathrm{a})} E_j + \chi_{ijkl}^{(\mathrm{a})} E_j \hat{M}_k \hat{M}_l + \ldots \tag{3}$$

Here, $\chi_{ij}^{(\mathrm{a})}$ is an axial tensor of second rank, $\chi_{ijkl}^{(\mathrm{a})}$ is an axial tensor of fourth rank and summation over repeated indices is implied. Note that the effective field of the odd torque is even in the magnetization: $\boldsymbol{B}^{\mathrm{odd}}(\hat{\boldsymbol{M}}) = \boldsymbol{B}^{\mathrm{odd}}(-\hat{\boldsymbol{M}})$ because of $\boldsymbol{T}^{\mathrm{odd}} = \mu\hat{\boldsymbol{M}} \times \boldsymbol{B}^{\mathrm{odd}}$ (in our notation the torque $\boldsymbol{T}$ carries the superscript odd, when it is odd in the magnetization, i.e., $\boldsymbol{T}^{\mathrm{odd}}(\hat{\boldsymbol{M}}) = -\boldsymbol{T}^{\mathrm{odd}}(-\hat{\boldsymbol{M}})$, while the effective magnetic field $\boldsymbol{B}$ carries the superscript odd, when it generates $\boldsymbol{T}^{\mathrm{odd}}$). In order to express the symmetry-allowed tensors $\chi_{ij}^{(\mathrm{a})}$ and $\chi_{ijkl}^{(\mathrm{a})}$ in terms of basis tensors we introduce the following notation to define these basis tensors:

$$\delta_{ij}^{(mn)} = \delta_{im}\delta_{jn} \rightarrow \langle mn \rangle \tag{4}$$

and

$$\delta_{ijkl}^{(mnop)} = \delta_{im}\delta_{jn}\delta_{ko}\delta_{lp} \rightarrow \langle mnop \rangle. \tag{5}$$

The superscripts (mn) and $(mnop)$ serve to label the basis tensors. As a simple example to illustrate the use of these basis tensors consider the unit matrix. The unit matrix can be expressed as follows:

$$\delta_{ij} = \delta_{ij}^{(11)} + \delta_{ij}^{(22)} + \delta_{ij}^{(33)}, \tag{6}$$

or simply $\langle 11 \rangle + \langle 22 \rangle + \langle 33 \rangle$. Similarly, any given tensor may be expressed in terms of these basis tensors. The symmetry-allowed form of the torkance tensor depends on the crystallographic point group [14,26]. Cubic, tetragonally-strained, and shear-strained PtMnSb possess different crystallographic point groups. Therefore, we discuss the symmetry-allowed form of the torkance tensor separately for these three cases in the following. Note that in Eq. (3) we expand the effective field only in terms of the applied electric field and in terms of the magnetization but we do not expand it in terms of the strain. This is a major difference to the treatment of e.g. the piezomagnetic effects in Ref. [26], where the strain itself is considered as a perturbation. Instead, we assume here that the strain is constant and that it determines the symmetry-allowed form of the response tensor by affecting the crystallographic point group.

TABLE I. List of axial tensors of ranks 2 and 4 allowed by symmetry in tetragonally strained half Heuslers. The notation introduced in Eq. (5) is used. Arrows indicate tensors that may be replaced by others due to permutations of indices, while (8) denotes tensors that may be replaced by others due to Eq. (8).

#	$\chi^{(\mathrm{a}\#)}$	#	$\chi^{(\mathrm{a}\#)}$	Remark
1	$\langle 22 \rangle - \langle 11 \rangle$	7	$\langle 3113 \rangle - \langle 3223 \rangle$	$\rightarrow \chi^{(\mathrm{a5})}$
2	$\langle 2112 \rangle - \langle 1221 \rangle$	8	$\langle 2323 \rangle - \langle 1313 \rangle$	$\rightarrow \chi^{(\mathrm{a6})}$
3	$\langle 1122 \rangle - \langle 2211 \rangle$	9	$\langle 2233 \rangle - \langle 1133 \rangle$	
4	$\langle 3322 \rangle - \langle 3311 \rangle$	10	$\langle 1212 \rangle - \langle 2121 \rangle$	$\rightarrow -\chi^{(\mathrm{a2})}$
5	$\langle 3131 \rangle - \langle 3232 \rangle$	11	$\langle 2222 \rangle - \langle 1111 \rangle$	(8)
6	$\langle 2332 \rangle - \langle 1331 \rangle$			

Tetragonal strain

First, we consider the case of tetragonal strain. The cases of shear strain and of cubic half Heuslers are discussed in Appendix A. For $a = b \neq c$ and $\alpha = \beta = \gamma = 90^\circ$ (point group $\bar{4}2m$) we list the 11 axial tensors of rank 2 and 4 that are allowed by symmetry in Table I. In Eq. (3) the indices k and l of $\chi_{ijkl}^{(a)}$ both couple to magnetization and are therefore interchangeable. Therefore, as indicated in Table I by arrows,

$$\chi_{ijkl}^{(\mathrm{a10})} = -\chi_{ijlk}^{(\mathrm{a2})}, \quad \chi_{ijkl}^{(\mathrm{a7})} = \chi_{ijlk}^{(\mathrm{a5})}, \quad \chi_{ijkl}^{(\mathrm{a8})} = \chi_{ijlk}^{(\mathrm{a6})}. \tag{7}$$

Moreover, we find

$$\left(\chi_{ijkl}^{(\mathrm{a3})} - \chi_{ijkl}^{(\mathrm{a9})} - \chi_{ijkl}^{(\mathrm{a11})}\right)\hat{M}_k\hat{M}_l = -\chi_{ij}^{(\mathrm{a1})}. \tag{8}$$

Thus, we do not need to consider the tensors 10, 7, 8 and 11 when we express $\chi^{(a)}_{ijkl}$ in terms of the tensors in Table I. Consequently, we can express the tensors in Eq. (3) as

$$\begin{aligned}\chi^{(a)}_{ij} &= \alpha_1 \chi^{(a1)}_{ij}\\ \chi^{(a)}_{ijkl} &= \alpha_2 \chi^{(a2)}_{ijkl} + \alpha_3 \chi^{(a3)}_{ijkl} + \alpha_4 \chi^{(a4)}_{ijkl} + \alpha_5 \chi^{(a5)}_{ijkl}\\ &\quad + \alpha_6 \chi^{(a6)}_{ijkl} + \alpha_7 \chi^{(a9)}_{ijkl}\end{aligned} \tag{9}$$

in terms of seven expansion coefficients $\alpha_1, \ldots, \alpha_7$. The tensor $\chi^{(a1)}_{ij} = \delta^{(22)}_{ij} - \delta^{(11)}_{ij}$ describes the effective SOT field from Dresselhaus SOI [12,14]. The tensors 2, 3, 4, 5, 6, and 9 describe higher-order contributions to the SOT, which have not yet been discussed in the literature.

The odd torque $\boldsymbol{T}^{\text{odd}}$ is related to its effective field by

$$T^{\text{odd}}_i = \Xi_{ij} B^{\text{odd}}_j, \tag{10}$$

where

$$\boldsymbol{\Xi} = \mu \begin{pmatrix} 0 & -\hat{M}_3 & \hat{M}_2 \\ \hat{M}_3 & 0 & -\hat{M}_1 \\ -\hat{M}_2 & \hat{M}_1 & 0 \end{pmatrix}. \tag{11}$$

Using Eqs. (3), (9), and (10) we obtain

$$\boldsymbol{T}^{\text{odd}} = \boldsymbol{t}^{\text{odd}} \boldsymbol{E}, \tag{12}$$

where

$$t^{\text{odd}}_{ij} = \mu \sum_{k=1}^{7} \alpha_k \vartheta^{(\text{odd}k)}_{ij} \tag{13}$$

with

$$\begin{aligned}
\vartheta^{(\text{odd1})} &= \begin{pmatrix} 0 & -\hat{M}_3 & 0 \\ -\hat{M}_3 & 0 & 0 \\ \hat{M}_2 & \hat{M}_1 & 0 \end{pmatrix},\\
\vartheta^{(\text{odd2})} &= \begin{pmatrix} -\hat{M}_1\hat{M}_2\hat{M}_3 & 0 & 0 \\ 0 & -\hat{M}_1\hat{M}_2\hat{M}_3 & 0 \\ \hat{M}_1^2\hat{M}_2 & \hat{M}_1\hat{M}_2^2 & 0 \end{pmatrix},\\
\vartheta^{(\text{odd3})} &= \begin{pmatrix} 0 & \hat{M}_1^2\hat{M}_3 & 0 \\ \hat{M}_2^2\hat{M}_3 & 0 & 0 \\ -\hat{M}_2^3 & -\hat{M}_1^3 & 0 \end{pmatrix},\\
\vartheta^{(\text{odd4})} &= \begin{pmatrix} 0 & 0 & \hat{M}_2^3 - \hat{M}_1^2\hat{M}_2 \\ 0 & 0 & \hat{M}_1^3 - \hat{M}_1\hat{M}_2^2 \\ 0 & 0 & 0 \end{pmatrix},\\
\vartheta^{(\text{odd5})} &= \begin{pmatrix} \hat{M}_1\hat{M}_2\hat{M}_3 & -\hat{M}_2^2\hat{M}_3 & 0 \\ -\hat{M}_1^2\hat{M}_3 & \hat{M}_1\hat{M}_2\hat{M}_3 & 0 \\ 0 & 0 & 0 \end{pmatrix},\\
\vartheta^{(\text{odd6})} &= \begin{pmatrix} 0 & 0 & -\hat{M}_2\hat{M}_3^2 \\ 0 & 0 & -\hat{M}_1\hat{M}_3^2 \\ 0 & 0 & 2\hat{M}_1\hat{M}_2\hat{M}_3 \end{pmatrix},\\
\vartheta^{(\text{odd7})} &= \begin{pmatrix} 0 & -\hat{M}_3^3 & 0 \\ -\hat{M}_3^3 & 0 & 0 \\ \hat{M}_3^2\hat{M}_2 & \hat{M}_1\hat{M}_3^2 & 0 \end{pmatrix}.
\end{aligned} \tag{14}$$

Since

$$\vartheta^{(\text{odd2})} + \vartheta^{(\text{odd5})} - \vartheta^{(\text{odd3})} + \vartheta^{(\text{odd7})} = \vartheta^{(\text{odd1})}, \tag{15}$$

we can set $\alpha_7 = 0$ in Eq. (13). Thus, the odd torkance tensor can be expressed in terms of 6 tensors $\vartheta^{(\text{odd1})}$, ..., $\vartheta^{(\text{odd6})}$:

$$t^{\text{odd}}_{ij} = \sum_{k=1}^{6} \beta_k \vartheta^{(\text{odd}k)}_{ij} \tag{16}$$

with expansion coefficients β_1, ..., β_6. By fitting Eq. (16) to the odd torque given for a set of magnetization directions, one may determine the coefficients β_i and subsequently use Eq. (16) to predict the odd torque for any magnetization direction.

B. Even torque

The effective field of the even torque can be expressed in terms of the electric field $\boldsymbol{E}$ and the magnetization direction $\hat{\boldsymbol{M}}$ as follows:

$$B^{\text{even}}_i = \chi^{(\text{p})}_{ijk} E_j \hat{M}_k + \chi^{(\text{p})}_{ijklm} E_j \hat{M}_k \hat{M}_l \hat{M}_m + \ldots. \tag{17}$$

Here, $\chi^{(\text{p})}_{ijk}$ is a polar tensor of third rank, $\chi^{(\text{p})}_{ijklm}$ is a polar tensor of fifth rank and summation over repeated indices is implied. Note that the effective field of the even torque is odd in the magnetization.

Tetragonal strain

Here, we discuss the case of tetragonal strain. The cases of shear strain and of cubic half Heuslers are discussed in Appendix B. For $a = b \neq c$ and $\alpha = \beta = \gamma = 90^\circ$ we list the polar tensors that are allowed by symmetry in Table II. In Eq. (17) the indices k, l and m of $\chi^{(\text{p})}_{ijklm}$ are contracted with the magnetization direction and are therefore interchangeable. Tensors that are related to other tensors by interchange of the indices k, l and m are specified in Table II by arrows. These tensors do not need to be considered when we expand $\chi^{(\text{p})}_{ijklm}$. When considering the permutations of the indices k, l and m the list of independent tensors that are needed in the expansion of $\chi^{(\text{p})}_{ijk}$ and $\chi^{(\text{p})}_{ijklm}$ is therefore reduced to the following ones: 1, 2, 3, 4, 6, 7, 8, 14, 15, 17, 23, 24, 25, 26.

Due to the relations

$$\begin{aligned}
\Xi_{ni}\big[\chi^{(\text{p4})}_{ijklm} + 2\chi^{(\text{p17})}_{ijklm}\big]\hat{M}_k\hat{M}_l\hat{M}_m &= 0,\\
\Xi_{ni}\big[\chi^{(\text{p6})}_{ijklm} + \chi^{(\text{p7})}_{ijklm} + \chi^{(\text{p25})}_{ijklm}\big]\hat{M}_k\hat{M}_l\hat{M}_m &= 0,\\
\big[\chi^{(\text{p7})}_{ijklm} + \chi^{(\text{p15})}_{ijklm} + \chi^{(\text{p23})}_{ijklm}\big]\hat{M}_k\hat{M}_l\hat{M}_m &= \chi^{(\text{p1})}_{ijk}\hat{M}_k,\\
\big[\chi^{(\text{p8})}_{ijklm} + \chi^{(\text{p17})}_{ijklm} + \chi^{(\text{p24})}_{ijklm}\big]\hat{M}_k\hat{M}_l\hat{M}_m &= \chi^{(\text{p2})}_{ijk}\hat{M}_k,\\
\big[\chi^{(\text{p14})}_{ijklm} + \chi^{(\text{p25})}_{ijklm} + \chi^{(\text{p26})}_{ijklm}\big]\hat{M}_k\hat{M}_l\hat{M}_m &= \chi^{(\text{p3})}_{ijk}\hat{M}_k,
\end{aligned} \tag{18}$$

we do not need to consider the tensors 17, 23, 24, 25, and 26. This leaves us with 3 polar tensors of rank 3 and 6 polar tensors of rank 5 to describe the SOT effective magnetic field in the tetragonal case, i.e., 9 tensors in total.

TABLE II. List of polar tensors of rank 3 and 5 allowed by symmetry in tetragonally strained half Heuslers. The notation introduced in Eq. (5) is used. Arrows indicate tensors that may be replaced by others due to permutation of indices, while (18) denotes tensors that may be replaced by others due to Eq. (18).

#	$\chi^{(\mathrm{p}\#)}$	Note	#	$\chi^{(\mathrm{p}\#)}$	Note
1	$\langle 321\rangle + \langle 312\rangle$		18	$\langle 13121\rangle + \langle 23212\rangle$	$\rightarrow 17$
2	$\langle 231\rangle + \langle 132\rangle$		19	$\langle 22321\rangle + \langle 11312\rangle$	$\rightarrow 6$
3	$\langle 213\rangle + \langle 123\rangle$		20	$\langle 11321\rangle + \langle 22312\rangle$	$\rightarrow 6$
4	$\langle 33231\rangle + \langle 33132\rangle$		21	$\langle 31211\rangle + \langle 32122\rangle$	$\rightarrow 15$
5	$\langle 33321\rangle + \langle 33312\rangle$	$\rightarrow 4$	22	$\langle 13211\rangle + \langle 23122\rangle$	$\rightarrow 17$
6	$\langle 22231\rangle + \langle 11132\rangle$		23	$\langle 32111\rangle + \langle 31222\rangle$	(18)
7	$\langle 32331\rangle + \langle 31332\rangle$		24	$\langle 23111\rangle + \langle 13222\rangle$	(18)
8	$\langle 23331\rangle + \langle 13332\rangle$		25	$\langle 12311\rangle + \langle 21322\rangle$	(18)
9	$\langle 33213\rangle + \langle 33123\rangle$	$\rightarrow 4$	26	$\langle 21311\rangle + \langle 12322\rangle$	(18)
10	$\langle 32313\rangle + \langle 31323\rangle$	$\rightarrow 7$	27	$\langle 11231\rangle + \langle 22132\rangle$	$\rightarrow 6$
11	$\langle 23313\rangle + \langle 13323\rangle$	$\rightarrow 8$	28	$\langle 12131\rangle + \langle 21232\rangle$	$\rightarrow 25$
12	$\langle 32133\rangle + \langle 31233\rangle$	$\rightarrow 7$	29	$\langle 21131\rangle + \langle 12232\rangle$	$\rightarrow 26$
13	$\langle 23133\rangle + \langle 13233\rangle$	$\rightarrow 8$	30	$\langle 22213\rangle + \langle 11123\rangle$	$\rightarrow 6$
14	$\langle 21333\rangle + \langle 12333\rangle$		31	$\langle 11213\rangle + \langle 22123\rangle$	$\rightarrow 6$
15	$\langle 31121\rangle + \langle 32212\rangle$		32	$\langle 12113\rangle + \langle 21223\rangle$	$\rightarrow 25$
16	$\langle 32221\rangle + \langle 31112\rangle$	$\rightarrow 15$	33	$\langle 21113\rangle + \langle 12223\rangle$	$\rightarrow 26$
17	$\langle 23221\rangle + \langle 13112\rangle$	(18)			

Using $\boldsymbol{T}^{\mathrm{even}} = \mu\hat{\boldsymbol{M}} \times \boldsymbol{B}^{\mathrm{even}}$, and $\boldsymbol{T}^{\mathrm{even}} = \boldsymbol{t}^{\mathrm{even}}\boldsymbol{E}$, we arrive at

$$t_{ij}^{\mathrm{even}} = \mu \sum_{k=1}^{9} \gamma_k \vartheta_{ij}^{(\mathrm{even}k)} \tag{19}$$

with

$$\vartheta^{(\mathrm{even1})} = \begin{pmatrix} \hat{M}_2^2 & \hat{M}_1\hat{M}_2 & 0 \\ -\hat{M}_1\hat{M}_2 & -\hat{M}_1^2 & 0 \\ 0 & 0 & 0 \end{pmatrix},$$

$$\vartheta^{(\mathrm{even2})} = \begin{pmatrix} 0 & 0 & -\hat{M}_1\hat{M}_3 \\ 0 & 0 & \hat{M}_2\hat{M}_3 \\ 0 & 0 & -\hat{M}_2^2 + \hat{M}_1^2 \end{pmatrix},$$

$$\vartheta^{(\mathrm{even3})} = \begin{pmatrix} -\hat{M}_3^2 & 0 & 0 \\ 0 & \hat{M}_3^2 & 0 \\ \hat{M}_1\hat{M}_3 & -\hat{M}_2\hat{M}_3 & 0 \end{pmatrix},$$

$$\vartheta^{(\mathrm{even4})} = \begin{pmatrix} 0 & 0 & 2\hat{M}_1\hat{M}_2^2\hat{M}_3 \\ 0 & 0 & -2\hat{M}_1^2\hat{M}_2\hat{M}_3 \\ 0 & 0 & 0 \end{pmatrix},$$

$$\vartheta^{(\mathrm{even5})} = \begin{pmatrix} 0 & -\hat{M}_1\hat{M}_2\hat{M}_3^2 & 0 \\ \hat{M}_1\hat{M}_2\hat{M}_3^2 & 0 & 0 \\ -\hat{M}_1\hat{M}_2^2\hat{M}_3 & \hat{M}_1^2\hat{M}_2\hat{M}_3 & 0 \end{pmatrix},$$

$$\vartheta^{(\mathrm{even6})} = \begin{pmatrix} \hat{M}_2^2\hat{M}_3^2 & \hat{M}_1\hat{M}_2\hat{M}_3^2 & 0 \\ -\hat{M}_1\hat{M}_2\hat{M}_3^2 & -\hat{M}_1^2\hat{M}_3^2 & 0 \\ 0 & 0 & 0 \end{pmatrix},$$

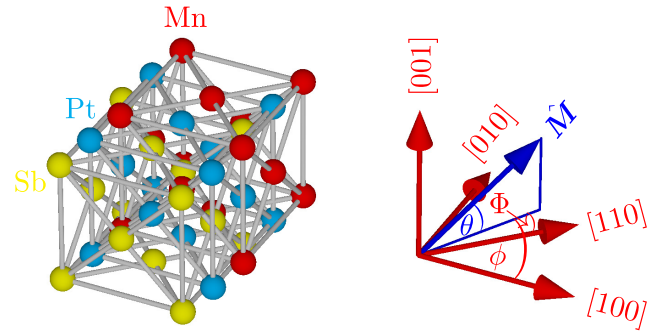

FIG. 1. Conventional unit cell of PtMnSb. The Pt, Mn, and Sb atoms each form an fcc lattice individually. The polar and azimuthal angles of the magnetization are denoted by θ and ϕ, respectively. By Φ we denote the angle $\Phi = \phi - 45^\circ$.

$$\vartheta^{(\mathrm{even7})} = \begin{pmatrix} 0 & 0 & -\hat{M}_3^3\hat{M}_1 \\ 0 & 0 & \hat{M}_3^3\hat{M}_2 \\ 0 & 0 & \hat{M}_1^2\hat{M}_3^2 - \hat{M}_2^2\hat{M}_3^2 \end{pmatrix},$$

$$\vartheta^{(\mathrm{even8})} = \begin{pmatrix} -\hat{M}_3^4 & 0 & 0 \\ 0 & \hat{M}_3^4 & 0 \\ \hat{M}_3^3\hat{M}_1 & -\hat{M}_3^3\hat{M}_2 & 0 \end{pmatrix},$$

$$\vartheta^{(\mathrm{even9})} = \begin{pmatrix} \hat{M}_1^2\hat{M}_2^2 & \hat{M}_2^3\hat{M}_1 & 0 \\ -\hat{M}_1^3\hat{M}_2 & -\hat{M}_1^2\hat{M}_2^2 & 0 \\ 0 & 0 & 0 \end{pmatrix}. \tag{20}$$

III. RESULTS

A. Computational details

We performed electronic structure calculations of PtMnSb based on the generalized gradient approximation (GGA) [27] as implemented in the FLEUR program [28]. The unit cell is shown in Fig. 1. In order to judge how sensitive the SOT is to the exchange correlation functional, we performed additional calculations within the local density approximation (LDA) [29]. We included SOI self-consistently using the second variation method [30]. To compute cubic PtMnSb we use the experimental lattice constant $a_{\mathrm{cub}} = c_{\mathrm{cub}} = 11.72a_0$ [20] in our calculations, where a_0 is Bohr's radius. We considered 4 systems with different tetragonal strains $\eta = (c - c_{\mathrm{cub}})/c_{\mathrm{cub}}$: $\eta = 1.45\%$ ($a = 11.49a_0$ and $c = 11.89a_0$), $\eta = 0.723\%$ ($a = 11.61a_0$ and $c = 11.81a_0$), $\eta = -0.723\%$ ($a = 11.84a_0$ and $c = 11.64a_0$), and $\eta = -1.45\%$ ($a = 11.95a_0$ and $c = 11.55a_0$). Additionally, we considered 7 systems with different shear strains $\epsilon = \gamma - 90^\circ$, where γ is the angle between the a axis and the b axis: $\epsilon = 2^\circ$, $\epsilon = 1^\circ$, $\epsilon = 0.5^\circ$, $\epsilon = 0.2^\circ$, $\epsilon = 0.1^\circ$, $\epsilon = -0.1^\circ$, $\epsilon = -0.2^\circ$

After obtaining the electronic structure self-consistently we generated maximally localized Wannier functions (MLWFs) using the Wannier90 code [31] in order to calculate the SOTs according to the method described in Ref. [25] with the help of Wannier interpolation for computational speed-up. We disentangled 44 MLWFs from 66 bands. For Mn and Pt we used sp^3d^2, d_{xy}, d_{yz} and d_{zx} trial orbitals. For Sb we employed s and p trial orbitals.

The even torkance is given by [25]

$$t_{ij}^{\text{even}} = \frac{e\hbar}{2\pi\mathcal{N}} \sum_{kn\neq m} \text{Im}[\langle\psi_{kn}|\mathcal{T}_i|\psi_{km}\rangle\langle\psi_{km}|v_j|\psi_{kn}\rangle] \times \left\{ \frac{\Gamma(\mathcal{E}_{km}-\mathcal{E}_{kn})}{[(\mathcal{E}_\text{F}-\mathcal{E}_{kn})^2+\Gamma^2][(\mathcal{E}_\text{F}-\mathcal{E}_{km})^2+\Gamma^2]} + \frac{2\Gamma}{[\mathcal{E}_{kn}-\mathcal{E}_{km}][(\mathcal{E}_\text{F}-\mathcal{E}_{km})^2+\Gamma^2]} + \frac{2}{[\mathcal{E}_{kn}-\mathcal{E}_{km}]^2}\text{Im}\log\frac{\mathcal{E}_{km}-\mathcal{E}_\text{F}-i\Gamma}{\mathcal{E}_{kn}-\mathcal{E}_\text{F}-i\Gamma} \right\} \quad (21)$$

and the odd torkance is given by

$$t_{ij}^{\text{odd}} = \frac{e\hbar}{\pi\mathcal{N}} \sum_{knm} \frac{\Gamma^2\text{Re}[\langle\psi_{kn}|\mathcal{T}_i|\psi_{km}\rangle\langle\psi_{km}|v_j|\psi_{kn}\rangle]}{[(\mathcal{E}_\text{F}-\mathcal{E}_{kn})^2+\Gamma^2][(\mathcal{E}_\text{F}-\mathcal{E}_{km})^2+\Gamma^2]}, \quad (22)$$

where $\mathcal{N}$ is the number of $\boldsymbol{k}$ points used to sample the Brillouin zone, e is the elementary positive charge, $\mathcal{T}_i$ is the i-th Cartesian component of the torque operator, v_j is the j-th Cartesian component of the velocity operator, Γ is the quasiparticle broadening, and ψ_{kn} and $\mathcal{E}_{kn}$ denote the Bloch function for band n at k point $\boldsymbol{k}$ and the corresponding band energy, respectively. A constant broadening of $\Gamma = 25$ meV was used in the calculations unless noted otherwise.

Due to the half-metallicity the spin magnetic moment per unit cell takes the integer value $\mu = 4\mu_\text{B}$ when SOI is not included in the calculations, where μ_B is Bohr's magneton. When we compute the magnetic moments contained in muffin-tin spheres around the atoms, we find that Mn contributes most to the total magnetic moment. In detail the atomic magnetic moments (in units of μ_B) obtained in GGA (LDA) are as follows: 3.91 (3.8) on Mn, 0.11 (0.14) on Pt, and −0.072 (−0.047) on Sb. In our calculations of SOT we include SOI and therefore the magnetic moment slightly deviates from the integer value $\mu = 4\mu_\text{B}$. This deviation depends on the strain and on the magnetization direction, but it is at most 1% for the strains that we consider. Therefore, $\mu \approx 4\mu_\text{B}$ is very well satisfied in all our calculations. When we present our *ab initio* results we use $ea_0 \approx 8.478 \times 10^{-30}$Cm as the unit of torkance. A torkance of one ea_0 corresponds therefore to an effective magnetic field of $B = ea_0E/\mu \approx 0.229\,\mu$T when the applied electric field is $E = 1$ V/m.

In Ref. [25] we have shown that the odd SOT is proportional to $1/\Gamma$ in the limit $\Gamma \to 0$, while the even SOT is independent of Γ in this limit. Therefore, it may be convenient to discuss the odd SOT per applied electric current, because this ratio is independent of Γ in the limit of $\Gamma \to 0$. The resistivity of cubic PtMnSb at $\Gamma = 25$ meV is given by $\rho_{xx} = 17\,\mu\Omega\,$cm, which we computed using the equations given in Ref. [25]. Consequently, an odd torkance of one ea_0 at $\Gamma = 25$ meV corresponds to an effective magnetic field per electric current-density ratio of $B/j = ea_0E/(\mu j) = ea_0\rho_{xx}/\mu \approx 3.89 \times 10^{-14}$ Tm^2/A.

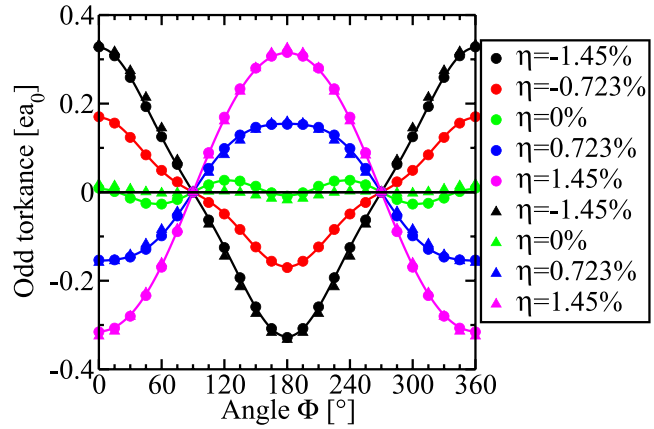

FIG. 2. Angular dependence of the odd torkance in PtMnSb for several strains $\eta = (c - c_\text{cub})/c_\text{cub}$ obtained in GGA (filled circles) and LDA (filled triangles) when the electric current is applied along the [110] direction and when the magnetization is in-plane. Φ is the angle between the magnetization and the [110] direction. The component of the odd torque pointing in the [001] direction is shown. Solid lines are fits to the GGA results according to Eq. (16).

B. Odd torque

In Fig. 2 we show the odd torkance as a function of the azimuthal angle of the magnetization for different tetragonal strains. Strain increases the odd torkance significantly. At large strain the odd SOT is of the same order of magnitude as in experiments on NiMnSb [13]. A suitable substrate on which PtMnSb[100] grows under tetragonal strain is W[100]. For W the theoretically estimated misfit strain is 2.1%, while the evaluation of diffraction data yields an estimated in-plane tensile strain of 0.31%–0.52% [20].

In the tetragonal systems the differences between the torkances computed with GGA (filled circles) and LDA (filled triangles) are very small. However, in the cubic system GGA and LDA differ even qualitatively: Here, the torkance has maxima close to 120° and close to 240° when GGA is used. However, when LDA is used it has a maximum at 0° instead. When we use Eq. (16) to fit the *ab initio* results we obtain very good agreement between the fit and the data, as shown in the figure.

In Fig. 3 we show the odd torkance as a function of the polar angle θ. It varies only moderately with the angle θ, in contrast to the strong variation with the angle ϕ shown in Fig. 2. When the tetragonal strain is η =1.45% the odd torkance is of the same order of magnitude as the even and odd torkances in magnetic bilayers such as Co/Pt and Mn/W [25].

In Fig. 4 we show the strain dependence of the parameters β_k in Eq. (16), which we use to fit the *ab initio* results. In cubic PtMnSb we find that relations Eq. (A8) are satisfied well. The coefficient β_1 varies linearly with strain and depends strongly on it, while the coefficients β_2 through β_6 are less sensitive to strain than β_1. In Eq. (16) β_1 is the coefficient of $\vartheta_{ij}^{(\text{odd1})}$, which describes the SOT from Dresselhaus-type SOI. However, β_1 does not vanish for zero strain. Of course, this does not imply that there is a Dresselhaus field at $\eta = 0$. Instead, it is simply a manifestation of Eq. (15), which shows

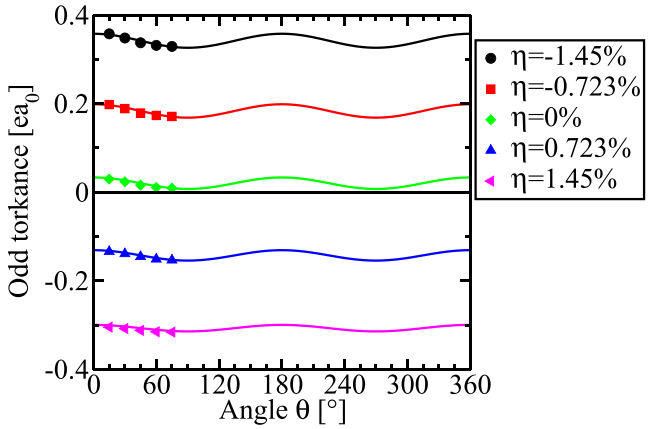

FIG. 3. Angular dependence of the odd torkance in PtMnSb for several strains $\eta = (c - c_{\text{cub}})/c_{\text{cub}}$ obtained in GGA when the electric current is applied in the [110] direction. The magnetization is rotated from the [001] direction (θ=0) to the [110] direction (θ = 90°). We show only the component of the torque that is parallel to the unit vector $\boldsymbol{e}_\theta$ of the spherical coordinate system. *Ab initio* data are shown by symbols, while solid lines are fits according to Eq. (16).

that $\vartheta_{ij}^{(\text{odd}1)}$ is not linearly independent from the higher order contributions described by the tensors 2, 3, 5, and 7.

In Eq. (16) we made the choice $\alpha_7 = 0$ in order to get an unambiguous representation of the torque in terms of a set of fitting parameters, which is only possible when we expand the torkance in terms of linearly independent tensors. However, it is possible to choose a different combination of tensors such that the coefficient of $\vartheta_{ij}^{(\text{odd}1)}$ is zero at $\eta = 0$. Such a combination has the advantage that one may claim that the coefficient of $\vartheta_{ij}^{(\text{odd}1)}$ corresponds to the Dresselhaus SOI. For this purpose we perform a second fitting run after determining the parameters β_1, ..., β_6 in Eq. (16) in the first fitting run. The second fitting run is based on

$$t_{ij}^{\text{odd}} = \sum_{k=1}^{7} \beta_k' \vartheta_{ij}^{(\text{odd}k)}, \tag{23}$$

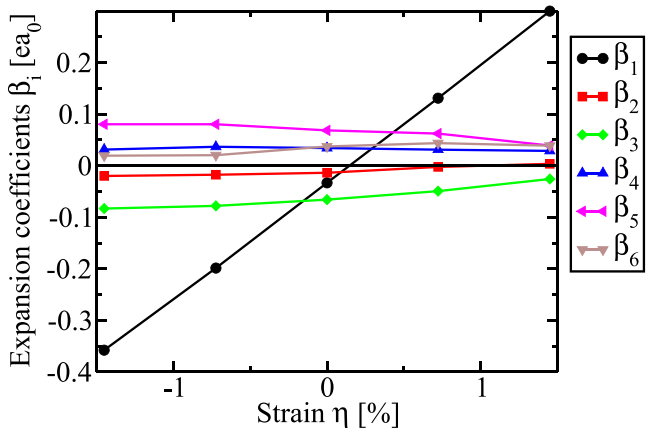

FIG. 4. PtMnSb: Expansion coefficients β_i in Eq. (16) for several strains $\eta = (c - c_{\text{cub}})/c_{\text{cub}}$ when the odd torkance is obtained from GGA.

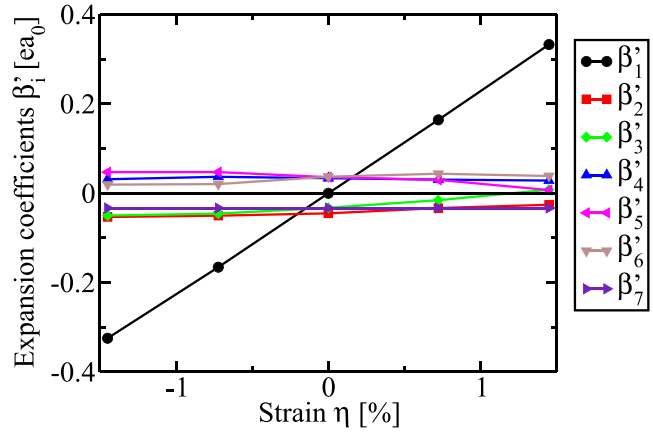

FIG. 5. PtMnSb: Expansion coefficients β_i' in Eq. (23) for several strains $\eta = (c - c_{\text{cub}})/c_{\text{cub}}$ when the odd torkance is obtained from GGA.

where we fix $\beta_7' = \beta_1(\eta = 0)$, while β_1', ..., β_6' are free fitting parameters. As shown in Fig. 5 this two-step fitting procedure leads to $\beta_1'(\eta = 0) = 0$, which can be understood easily from Eq. (15). We can thus claim that β_1' describes the SOT from the Dresselhaus field.

In Fig. 6 we show the expansion coefficients for the SOT obtained from LDA. Interestingly, the β_1' in Figs. 5 and 6 differ by less than 1%. Thus, the differences between LDA and GGA, which are illustrated in Fig. 2, are reflected mostly by the differences in the higher-order coefficients β_2', ..., β_7'. These higher-order coefficients differ significantly between GGA and LDA. However, for sufficiently large strain the contribution of the higher-order terms is relatively small compared with the Dresselhaus SOT described by β_1'. Therefore, the odd SOT is insensitive to the choice of the exchange correlation potential in strained PtMnSb, as discussed already in Fig. 2.

Next, we discuss the effect of shear strain ϵ on the odd torque. In Fig. 7 we show the odd torkance as a function of the azimuthal angle ϕ in the shear strained crystal. The enhancement of the odd SOT with shear strain is similarly strong as

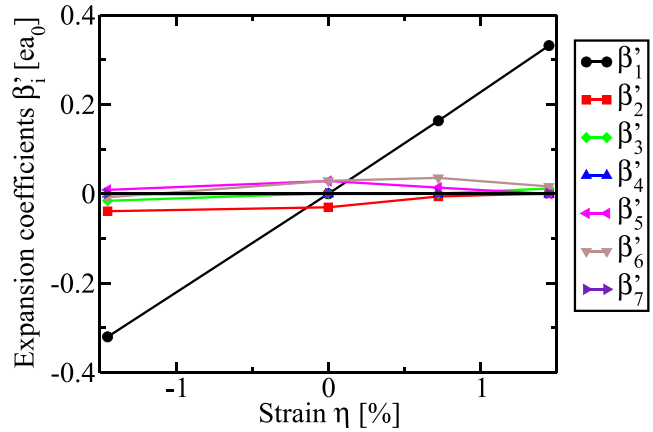

FIG. 6. PtMnSb: Expansion coefficients β_i' in Eq. (23) for several strains $\eta = (c - c_{\text{cub}})/c_{\text{cub}}$ when the odd torkance is obtained from LDA.

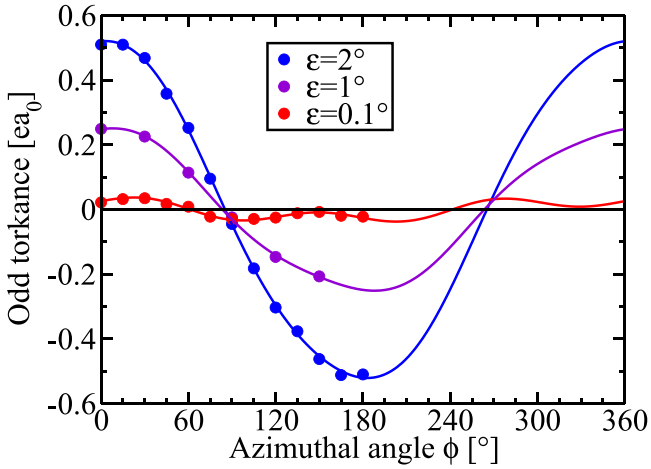

FIG. 7. Odd torkance in shear-strained PtMnSb obtained in GGA. The current direction is along [100]. The magnetization is in-plane. ϕ is the angle between the magnetization and the [100] direction. *Ab initio* data are shown by filled circles, while solid lines are fits according to Eq. (A9).

the enhancement with tetragonal strain. When the shear strain is $\epsilon = 2^\circ$ the odd torkance is of the same order of magnitude as the even and odd torkances in magnetic bilayers such as Co/Pt and Mn/W [25]. The variation of the odd torkance with azimuthal angle ϕ is similar to the angular dependence in tetragonally strained PtMnSb shown in Fig. 2.

At $\epsilon = 2^\circ$ the odd torkance exhibits a maximum at $\phi = 0^\circ$. In order to investigate the dependence of this maximum on ϵ we show in Fig. 8 the odd torkance at $\phi = 0^\circ$ as a function of ϵ. In the considered range the dependence on ϵ is approximately linear.

In Fig. 9 we show the expansion coefficients β_i in Eq. (A9) of the odd torkance. At large shear strain β_1 dominates clearly over the other contributions, i.e., the SOT from Rashba SOI is dominant. Since shear strain automatically implies tetragonal strain, a SOT from Dresselhaus SOI – described by β_2 – is

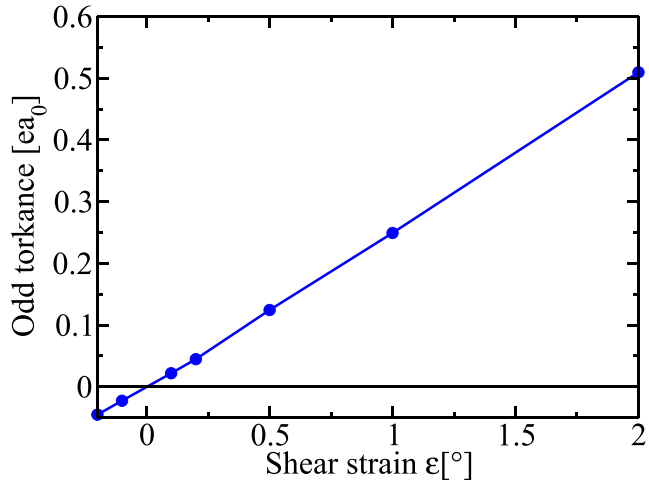

FIG. 8. Dependence of the odd torkance on shear-strain in PtMnSb when the polar and azimuthal angles of magnetization are $\theta = 90^\circ$ and $\phi = 0^\circ$, respectively.

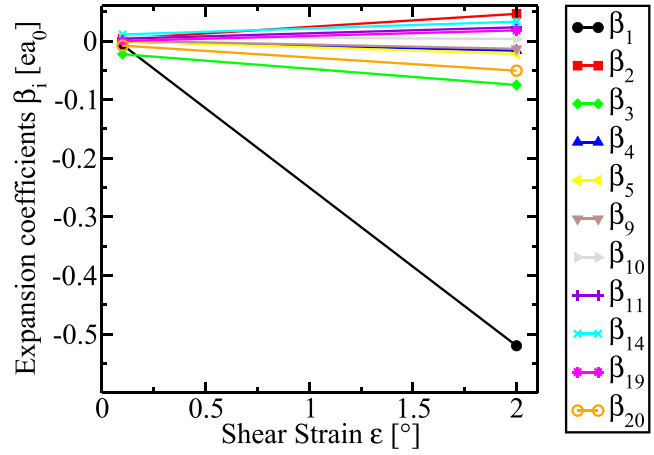

FIG. 9. Expansion coefficients β_i in Eq. (A9) of the odd torkance in shear-strained PtMnSb obtained in GGA.

present as well, but it is small compared to the SOT from Rashba SOI.

C. Even Torque

In Fig. 10 we show the even torkance as a function of the azimuthal angle Φ for several tetragonal strains η. The even torque is considerably less sensitive to strain than the odd torque. Additionally, at $\eta = 1.45\%$ the maximum even torkance is smaller than the maximum odd torkance by a factor of 12.5. In contrast to magnetic bilayer systems such as Co/Pt [15], where the even SOT is typically more important than the odd SOT, in PtMnSb the odd SOT dominates.

In Fig. 11 we show the even torkance in shear-strained PtMnSb at $\Gamma = 100$ meV. While the even torkance is more

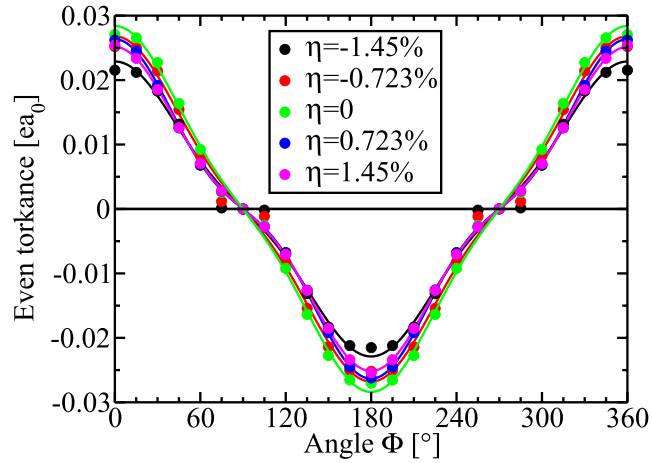

FIG. 10. Angular dependence of the even torkance obtained within GGA in PtMnSb for several tetragonal strains $\eta = (c - c_{\text{cub}})/c_{\text{cub}}$ when the electric current is applied along [110] direction and when the magnetization is in-plane. Φ is the angle between magnetization and the [110] direction. We show the component of the even torque that is parallel to the unit vector e_ϕ of the spherical coordinate system. *Ab-initio* data are shown by filled circles, while solid lines are fits according to Eq. (19).

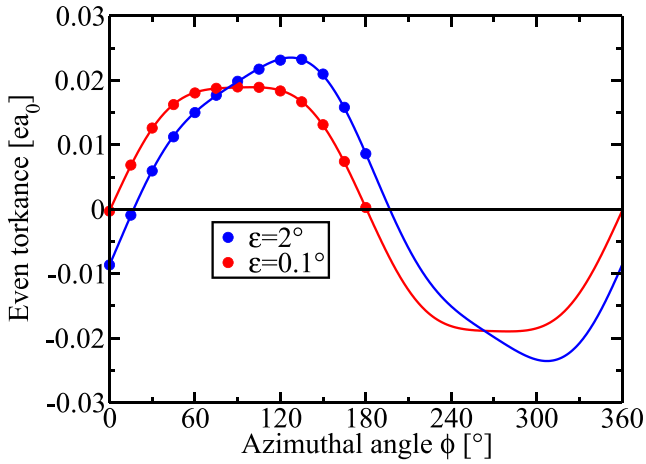

FIG. 11. Angular dependence of the even torkance obtained within GGA in PtMnSb for several shear strains ϵ when the electric current is applied along the [100] direction and when the magnetization is in-plane. ϕ is the angle between magnetization and the [100] direction. We show the component of the even torque that is parallel to the unit vector e_ϕ of the spherical coordinate system. *Ab initio* data are shown by filled circles, while solid lines are fits according to Eq. (B2).

sensitive to shear strain than to tetragonal strain, it is less sensitive to shear stain than the odd torkance.

IV. SUMMARY

We discuss the constraints that crystal symmetry imposes on the form of the SOT torkance tensor in half Heuslers with tetragonal or shear strain. We discuss the lowest order tensors, which correspond to Rashba and Dresselhaus SOI, but also higher order tensors. We perform first-principles DFT calculations of the SOT in half-Heusler PtMnSb as a function of tetragonal and shear strain. The odd torkance in PtMnSb depends strongly on tetragonal strain, which we attribute to the Dresselhaus SOI. We find the SOT from Dresselhaus SOI to be insensitive to the exchange-correlation functional, i.e., the differences between GGA and LDA are negligible. In contrast, the higher-order tensors differ substantially between GGA and LDA. However, these higher-order contributions are small in PtMnSb with tetragonal strain, such that the total odd torque in PtMnSb is insensitive to the exchange-correlation functional. The even torkance depends only weakly on tetragonal strain, but it depends moderately strongly on shear strain. The dependence of the odd SOT on shear strain is similarly strong as its dependence on tetragonal strain and it arises mostly from the Rashba SOI. In SOT applications PtMnSb should be grown on suitable substrates that maximize strain in order to obtain large torkances. Our results show that in strained PtMnSb torkances of the same order of magnitude as in NiMnSb experiments may be achieved.

ACKNOWLEDGMENTS

We acknowledge financial support from Leibniz Collaborative Excellence project OptiSPIN – Optical Control of Nanoscale Spin Textures, and funding under SPP 2137 "Skyrmionics" of the DFG. We gratefully acknowledge financial support from the European Research Council (ERC) under the European Union's Horizon 2020 research and innovation program (Grant No. 856538, project "3D MAGiC"). The work was also supported by the Deutsche Forschungsgemeinschaft (DFG, German Research Foundation) – TRR 173 – 268565370 (Project A11), TRR 288 – 422213477 (Project B06). We also gratefully acknowledge the Jülich Supercomputing Centre and RWTH Aachen University for providing computational resources under Project No. jiff40.

APPENDIX A: SYMMETRY ANALYSIS FOR THE ODD TORQUE IN CUBIC HALF HEUSLERS AND IN HALF HEUSLERS UNDER SHEAR STRAIN

a. Cubic PtMnSb

In the following we discuss the odd torque for the case of cubic half Heuslers, i.e., $a = b = c$ and $\alpha = \beta = \gamma = 90^\circ$ (point group $\bar{4}3m$). In contrast to the case with tetragonal strain, symmetry does not allow axial tensors of rank 2 in cubic PtMnSb [14]. The following axial tensors of rank 4 are allowed by symmetry:

$$\begin{aligned}
\chi^{(\mathrm{a12})}_{ijkl} &= \delta^{(2121)}_{ijkl} - \delta^{(1212)}_{ijkl} - \delta^{(3131)}_{ijkl} + \delta^{(3232)}_{ijkl} + \delta^{(1313)}_{ijkl} \\
&\quad - \delta^{(2323)}_{ijkl}, \\
\chi^{(\mathrm{a13})}_{ijkl} &= -\delta^{(2211)}_{ijkl} + \delta^{(1122)}_{ijkl} + \delta^{(3311)}_{ijkl} - \delta^{(3322)}_{ijkl} \\
&\quad - \delta^{(1133)}_{ijkl} + \delta^{(2233)}_{ijkl}, \\
\chi^{(\mathrm{a14})}_{ijkl} &= -\delta^{(1221)}_{ijkl} + \delta^{(2112)}_{ijkl} + \delta^{(1331)}_{ijkl} - \delta^{(2332)}_{ijkl} - \delta^{(3113)}_{ijkl} \\
&\quad + \delta^{(3223)}_{ijkl}.
\end{aligned} \tag{A1}$$

Since the indices k and l of χ_{ijkl} both couple to magnetization in Eq. (3) and since

$$\chi^{(\mathrm{a12})}_{ijkl}\hat{M}_k\hat{M}_l = \chi^{(\mathrm{a14})}_{ijkl}\hat{M}_k\hat{M}_l, \tag{A2}$$

we do not need to consider $\chi^{(\mathrm{a14})}$ when we expand $\chi^{(\mathrm{a})}_{ijkl}$ in terms of the tensors in Eq. (A1). Comparison of these tensors to Table I yields

$$\begin{aligned}
\chi^{(\mathrm{a12})}_{ijkl} &= \chi^{(\mathrm{a2})}_{ijlk} - \chi^{(\mathrm{a5})}_{ijkl} - \chi^{(\mathrm{a6})}_{ijlk}, \\
\chi^{(\mathrm{a13})}_{ijkl} &= \chi^{(\mathrm{a3})}_{ijkl} - \chi^{(\mathrm{a4})}_{ijkl} + \chi^{(\mathrm{a9})}_{ijkl}.
\end{aligned} \tag{A3}$$

Thus, for the cubic half Heuslers, we can express the tensors in Eq. (3) as follows:

$$\chi^{(\mathrm{a})}_{ij} = 0, \quad \chi^{(\mathrm{a})}_{ijkl} = \alpha_{12}\chi^{(\mathrm{a12})}_{ijkl} + \alpha_{13}\chi^{(\mathrm{a13})}_{ijkl}, \tag{A4}$$

with two coefficients α_{12} and α_{13} [14].

The corresponding torkance is given by

$$t^{\mathrm{odd}}_{ij} = \mu \sum_{k=12}^{13} \alpha_k \ \vartheta^{(\mathrm{odd}k)}_{ij} = \sum_{k=12}^{13} \beta_k \ \vartheta^{(\mathrm{odd}k)}_{ij} \tag{A5}$$

with

$$\vartheta^{(\mathrm{odd12})} = \vartheta^{(\mathrm{odd2})} - \vartheta^{(\mathrm{odd5})} - \vartheta^{(\mathrm{odd6})} = \begin{pmatrix} -2\hat{M}_1\hat{M}_2\hat{M}_3 & \hat{M}_2^2\hat{M}_3 & \hat{M}_2\hat{M}_3^2 \\ \hat{M}_1^2\hat{M}_3 & -2\hat{M}_1\hat{M}_2\hat{M}_3 & \hat{M}_1\hat{M}_3^2 \\ \hat{M}_1^2\hat{M}_2 & \hat{M}_1\hat{M}_2^2 & -2\hat{M}_1\hat{M}_2\hat{M}_3 \end{pmatrix} \tag{A6}$$

and

$$\vartheta^{(\mathrm{odd13})} = \vartheta^{(\mathrm{odd3})} - \vartheta^{(\mathrm{odd4})} + \vartheta^{(\mathrm{odd7})} = \begin{pmatrix} 0 & \hat{M}_1^2\hat{M}_3 - \hat{M}_3^3 & -\hat{M}_2^3 + \hat{M}_1^2\hat{M}_2 \\ \hat{M}_2^2\hat{M}_3 - \hat{M}_3^3 & 0 & -\hat{M}_1^3 + \hat{M}_1\hat{M}_2^2 \\ -\hat{M}_2^3 + \hat{M}_3^2\hat{M}_2 & -\hat{M}_1^3 + \hat{M}_1\hat{M}_3^2 & 0 \end{pmatrix}. \tag{A7}$$

Instead of using Eq. (A5) to fit the odd torkance in cubic PtMnSb, one can of course also use Eq. (16). By equating Eqs. (A5) and (16) we find that in cubic PtMnSb the following relations should be satisfied:

$$\begin{aligned} \beta_1 &= -\beta_4, \quad 2\beta_1 = \beta_3, \\ 2\beta_1 &= -\beta_2 - \beta_5, \quad \beta_6 = \beta_1 + \beta_5. \end{aligned} \tag{A8}$$

b. Shear strain

Finally, we discuss the odd torque in the presence of shear strain.

We present the axial tensors of rank 2 and rank 4 that are allowed by symmetry in shear-strained half-Heuslers in Table III. As indicated by arrows in the Table, tensors 6, 7, 15, 16, 17, and 18 do not need to be considered because both indices k and l of $\chi^{(a)}_{ijkl}$ couple to magnetization in Eq. (3) and these tensors may therefore be replaced by others. Additionally, tensor 8 does not need to be considered, because it evaluates to zero when both indices k and l of $\chi^{(a)}_{ijkl}$ are contracted with the magnetization. Tensor 1 describes the SOT effective field from Rashba SOI, tensor 2 describes the SOT effective field from Dresselhaus SOI [14], and the remaining tensors describe higher-order contributions that have not yet been discussed in the literature. Tensor 2 appears also in the case of tetragonal strain, see the first tensor in Table I. This is expected, because shear strain is automatically accompanied by tetragonal strain.

TABLE III. List of axial tensors of rank 2 and 4 allowed by symmetry in shear-strained half Heuslers. The notation introduced in Eq. (5) is used. Arrows indicate tensors that may be replaced by others due to permutation of indices, while (A10) denotes tensors that may be replaced by others due to Eq. (A10).

#	$\chi^{(\mathrm{a}\#)}$	Note	#	$\chi^{(\mathrm{a}\#)}$	Note
1	$\langle 21\rangle - \langle 12\rangle$		12	$\langle 3132\rangle - \langle 3231\rangle$	(A10)
2	$\langle 22\rangle - \langle 11\rangle$		13	$\langle 3232\rangle - \langle 3131\rangle$	(A10)
3	$\langle 2121\rangle - \langle 1212\rangle$		14	$\langle 2332\rangle - \langle 1331\rangle$	
4	$\langle 2221\rangle - \langle 1112\rangle$		15	$\langle 2313\rangle - \langle 1323\rangle$	$\to 5$
5	$\langle 2331\rangle - \langle 1332\rangle$		16	$\langle 3123\rangle - \langle 3213\rangle$	$\to 12$
6	$\langle 2112\rangle - \langle 1221\rangle$	$\to 3$	17	$\langle 3223\rangle - \langle 3113\rangle$	$\to 13$
7	$\langle 2212\rangle - \langle 1121\rangle$	$\to 4$	18	$\langle 2323\rangle - \langle 1313\rangle$	$\to 14$
8	$\langle 3312\rangle - \langle 3321\rangle$	$\emptyset$	19	$\langle 2133\rangle - \langle 1233\rangle$	
9	$\langle 2122\rangle - \langle 1211\rangle$		20	$\langle 2233\rangle - \langle 1133\rangle$	
10	$\langle 2222\rangle - \langle 1111\rangle$		21	$\langle 2111\rangle - \langle 1222\rangle$	(A10)
11	$\langle 3322\rangle - \langle 3311\rangle$		22	$\langle 2211\rangle - \langle 1122\rangle$	(A10)

The corresponding torkance may be written as

$$t^{\mathrm{odd}}_{ij} = \sum_{\#=1}^{2} \beta_\# \Xi_{im}\chi^{(\mathrm{a}\#)}_{mj} + \sum_{\#=3}^{22} \beta_\# \Xi_{im}\chi^{(\mathrm{a}\#)}_{mjkl}\hat{M}_k\hat{M}_l, \tag{A9}$$

where the matrix $\boldsymbol{\Xi}$ is defined in Eq. (11). As discussed above, one may set $\beta_\# = 0$ for all tensors # indicated by an arrow or by $\emptyset$ in Table III, i.e., $\beta_6 = 0$, $\beta_7 = 0$, $\beta_8 = 0$, $\beta_{15} = 0, \ldots$. However, due to the relations

$$\begin{aligned} \Xi_{im}\chi^{(\mathrm{a1})}_{mj} &= \Xi_{im}\chi^{(\mathrm{a4})}_{mjkl}\hat{M}_k\hat{M}_l - \Xi_{im}\chi^{(\mathrm{a12})}_{mjkl}\hat{M}_k\hat{M}_l \\ &\quad + \Xi_{im}\chi^{(\mathrm{a19})}_{mjkl}\hat{M}_k\hat{M}_l + \Xi_{im}\chi^{(\mathrm{a21})}_{mjkl}\hat{M}_k\hat{M}_l, \\ \Xi_{im}\chi^{(\mathrm{a2})}_{mj} &= \Xi_{im}\chi^{(\mathrm{a10})}_{mjkl}\hat{M}_k\hat{M}_l + \Xi_{im}\chi^{(\mathrm{a20})}_{mjkl}\hat{M}_k\hat{M}_l \\ &\quad + \Xi_{im}\chi^{(\mathrm{a22})}_{mjkl}\hat{M}_k\hat{M}_l, \\ \Xi_{im}\chi^{(\mathrm{a3})}_{mj} &= \Xi_{im}\chi^{(\mathrm{a10})}_{mjkl}\hat{M}_k\hat{M}_l + \Xi_{im}\chi^{(\mathrm{a13})}_{mjkl}\hat{M}_k\hat{M}_l, \\ \Xi_{im}\big[\chi^{(\mathrm{a4})}_{mjkl} &- \Xi_{im}\chi^{(\mathrm{a9})}_{mjkl} - \Xi_{im}\chi^{(\mathrm{a12})}_{mjkl}\big]\hat{M}_k\hat{M}_l = 0, \end{aligned} \tag{A10}$$

the remaining tensors in Eq. (A9) are not linearly independent. Therefore, we may additionally choose $\beta_{21} = 0$, $\beta_{22} = 0$, $\beta_{13} = 0$, and $\beta_{12} = 0$. Thus, only 11 independent tensors need to be considered in Eq. (A9) with 11 corresponding fitting parameters $\beta_\#$.

APPENDIX B: SYMMETRY ANALYSIS FOR THE EVEN TORQUE IN CUBIC HALF HEUSLERS AND IN HALF HEUSLERS UNDER SHEAR STRAIN

a. Cubic PtMnSb

When $a = b = c$ and $\alpha = \beta = \gamma = 90^\circ$, symmetry allows 11 polar tensors of rank 3 and rank 5, which we list in Table IV.

In Eq. (17) the last three indices are contracted with the magnetization. Therefore, for the purpose of application in Eq. (17), $\chi^{(\mathrm{p6})}_{ijklm}$ is equivalent with $\chi^{(\mathrm{p2})}_{ijklm}$, $\chi^{(\mathrm{p4})}_{ijklm}$ is equivalent with $\chi^{(\mathrm{p3})}_{ijklm}$, and $\chi^{(\mathrm{p9})}_{ijklm}$ is equivalent with $\chi^{(\mathrm{p8})}_{ijklm}$, as indicated in the Table. Consequently, we do not need to consider $\chi^{(\mathrm{p6})}_{ijklm}$, $\chi^{(\mathrm{p4})}_{ijklm}$, and $\chi^{(\mathrm{p9})}_{ijklm}$. Thus, the contribution to the effective field of the even SOT which is third order in $\hat{\boldsymbol{M}}$ can be expressed in

TABLE IV. List of polar tensors of rank 3 and 5 allowed by symmetry in cubic half Heuslers. The notation introduced in Eq. (5) is used. Arrows indicate tensors that may be replaced by others.

#	$\chi^{(\mathrm{p}\#)}$	Note
1	$\langle 321\rangle + \langle 231\rangle + \langle 312\rangle + \langle 132\rangle + \langle 213\rangle + \langle 123\rangle$	
2	$-\langle 13121\rangle - \langle 12131\rangle - \langle 23212\rangle - \langle 21232\rangle - \langle 32313\rangle - \langle 31323\rangle$	
3	$\langle 32221\rangle + \langle 23331\rangle + \langle 31112\rangle + \langle 13332\rangle + \langle 21113\rangle + \langle 12223\rangle$	
4	$\langle 31211\rangle + \langle 21311\rangle + \langle 32122\rangle + \langle 12322\rangle + \langle 23133\rangle + \langle 13233\rangle$	$\rightarrow \chi^{(\mathrm{p3})}$
5	$\langle 32111\rangle + \langle 23111\rangle + \langle 31222\rangle + \langle 13222\rangle + \langle 21333\rangle + \langle 12333\rangle$	
6	$\langle 13211\rangle + \langle 12311\rangle + \langle 23122\rangle + \langle 21322\rangle + \langle 32133\rangle + \langle 31233\rangle$	$\rightarrow \chi^{(\mathrm{p2})}$
7	$\langle 23221\rangle + \langle 32331\rangle + \langle 13112\rangle + \langle 31332\rangle + \langle 12113\rangle + \langle 21223\rangle$	
8	$\langle 11321\rangle + \langle 11231\rangle + \langle 22312\rangle + \langle 22132\rangle + \langle 33213\rangle + \langle 33123\rangle$	
9	$-\langle 33321\rangle - \langle 22231\rangle - \langle 33312\rangle - \langle 11132\rangle - \langle 22213\rangle - \langle 11123\rangle$	$\rightarrow \chi^{(\mathrm{p8})}$
10	$-\langle 31121\rangle - \langle 21131\rangle - \langle 32212\rangle - \langle 12232\rangle - \langle 23313\rangle - \langle 13323\rangle$	
11	$-\langle 22321\rangle - \langle 33231\rangle - \langle 11312\rangle - \langle 33132\rangle - \langle 11213\rangle - \langle 22123\rangle$	

terms of the tensor

$$\chi^{(\mathrm{p})}_{ijklm} = \alpha_2 \chi^{(\mathrm{p2})}_{ijklm} + \alpha_3 \chi^{(\mathrm{p3})}_{ijklm} + \alpha_5 \chi^{(\mathrm{p5})}_{ijklm} + \alpha_7 \chi^{(\mathrm{p7})}_{ijklm} + \alpha_8 \chi^{(\mathrm{p8})}_{ijklm} + \alpha_{10} \chi^{(\mathrm{p10})}_{ijklm} + \alpha_{11} \chi^{(\mathrm{p11})}_{ijklm}. \quad \text{(B1)}$$

b. Shear strain

Finally, we consider the case of shear strain. In Table V we present the polar tensors of rank 3 and 5 allowed by symmetry in shear-strained half Heuslers. As indicated in the Table by arrows, several tensors may be replaced by others, because in Eq. (17) the indices k, l, and m of $\chi^{(\mathrm{p})}_{ijklm}$ are interchangeable.

The corresponding torkance may be written as

$$t^{\mathrm{even}}_{ij} = \Xi_{in}\left[\sum_{\#=1}^{7} \beta_{\#} \chi^{(\mathrm{p}\#)}_{njk} + \sum_{\#=8}^{68} \beta_{\#} \chi^{(\mathrm{p}\#)}_{njklm} \hat{M}_l \hat{M}_m\right] \hat{M}_k, \quad \text{(B2)}$$

where the matrix $\boldsymbol{\Xi}$ is defined in Eq. (11). As discussed above, one may set $\beta_{\#} = 0$ for all tensors # indicated by an arrow in Table III, i.e., $\beta_{12} = 0$, $\beta_{13} = 0$, $\beta_{17} = 0, \ldots$.

Due to the relations

$$\begin{aligned}
\Xi_{in}\chi^{(\mathrm{p1})}_{njk}\hat{M}_k &= \Xi_{in}\big[\chi^{(\mathrm{p51})}_{njklm} + \chi^{(\mathrm{p62})}_{njklm}\big]\hat{M}_k\hat{M}_l\hat{M}_m,\\
\Xi_{in}\chi^{(\mathrm{p1})}_{njk}\hat{M}_k &= -\Xi_{in}\chi^{(\mathrm{p5})}_{njklm}\hat{M}_k\hat{M}_l\hat{M}_m,\\
0 &= \Xi_{in}\big[\chi^{(\mathrm{p27})}_{njklm} + \chi^{(\mathrm{p62})}_{njklm}\big]\hat{M}_k\hat{M}_l\hat{M}_m,\\
0 &= \Xi_{in}\big[\chi^{(\mathrm{p16})}_{njklm} + \tfrac{1}{2}\chi^{(\mathrm{p46})}_{njklm}\big]\hat{M}_k\hat{M}_l\hat{M}_m,\\
0 &= \Xi_{in}\big[\chi^{(\mathrm{p1})}_{njk} + \big[\chi^{(\mathrm{p15})}_{njklm} + \chi^{(\mathrm{p20})}_{njklm} + \chi^{(\mathrm{p27})}_{njklm}\big]\\
&\quad \times \hat{M}_l\hat{M}_m\big]\hat{M}_k,\\
0 &= \Xi_{in}\big[\chi^{(\mathrm{p2})}_{njk} - \big[\chi^{(\mathrm{p14})}_{njklm} + \chi^{(\mathrm{p63})}_{njklm} - \tfrac{1}{2}\chi^{(\mathrm{p46})}_{njklm}\big]\\
&\quad \times \hat{M}_l\hat{M}_m\big]\hat{M}_k,\\
0 &= \Xi_{in}\big[\chi^{(\mathrm{p3})}_{njk} - \big[\chi^{(\mathrm{p42})}_{njklm} + \chi^{(\mathrm{p49})}_{njklm} + \chi^{(\mathrm{p54})}_{njklm}\big]\hat{M}_l\hat{M}_m\big]\\
&\quad \times \hat{M}_k,\\
0 &= \Xi_{in}\big[\chi^{(\mathrm{p3})}_{njk} + \big[\chi^{(\mathrm{p9})}_{njklm} + \chi^{(\mathrm{p21})}_{njklm} - \chi^{(\mathrm{p42})}_{njklm}\\
&\quad - \chi^{(\mathrm{p49})}_{njklm}\big]\hat{M}_l\hat{M}_m\big]\hat{M}_k,
\end{aligned}$$

TABLE V. List of polar tensors of rank 3 and 5 allowed by symmetry in shear-strained half Heuslers. The notation introduced in Eq. (5) is used. Arrows indicate tensors that may be replaced by others due to permutations of indices, while tensors indicated by (B3) may be replaced by others due to Eq. (B3).

#	$\chi^{(\mathrm{p}\#)}$	Note	#	$\chi^{(\mathrm{p}\#)}$	Note
1	$\langle 333\rangle$		35	$\langle 12113\rangle + \langle 21223\rangle$	$\rightarrow 21$
2	$\langle 231\rangle + \langle 132\rangle$		36	$\langle 11113\rangle + \langle 22223\rangle$	$\rightarrow 22$
3	$\langle 321\rangle + \langle 312\rangle$		37	$\langle 13313\rangle + \langle 23323\rangle$	$\rightarrow 27$
4	$\langle 311\rangle + \langle 322\rangle$		38	$\langle 23133\rangle + \langle 13233\rangle$	$\rightarrow 14$
5	$\langle 131\rangle + \langle 232\rangle$	(B3)	39	$\langle 13133\rangle + \langle 23233\rangle$	$\rightarrow 27$
6	$\langle 213\rangle + \langle 123\rangle$		40	$\langle 21333\rangle + \langle 12333\rangle$	(B3)
7	$\langle 113\rangle + \langle 223\rangle$		41	$\langle 11333\rangle + \langle 22333\rangle$	(B3)
8	$\langle 21321\rangle + \langle 12312\rangle$		42	$\langle 32221\rangle + \langle 31112\rangle$	
9	$\langle 22321\rangle + \langle 11312\rangle$		43	$\langle 31221\rangle + \langle 32112\rangle$	
10	$\langle 21131\rangle + \langle 12232\rangle$		44	$\langle 32121\rangle + \langle 31212\rangle$	$\rightarrow 43$
11	$\langle 22131\rangle + \langle 11232\rangle$		45	$\langle 31121\rangle + \langle 32212\rangle$	$\rightarrow 42$
12	$\langle 21231\rangle + \langle 12132\rangle$	$\rightarrow 8$	46	$\langle 33321\rangle + \langle 33312\rangle$	(B3)
13	$\langle 22231\rangle + \langle 11132\rangle$	$\rightarrow 9$	47	$\langle 32211\rangle + \langle 31122\rangle$	$\rightarrow 43$
14	$\langle 23331\rangle + \langle 13332\rangle$		48	$\langle 31211\rangle + \langle 32122\rangle$	$\rightarrow 42$
15	$\langle 13221\rangle + \langle 23112\rangle$		49	$\langle 32111\rangle + \langle 31222\rangle$	(B3)
16	$\langle 13121\rangle + \langle 23212\rangle$		50	$\langle 31111\rangle + \langle 32222\rangle$	(B3)
17	$\langle 12321\rangle + \langle 21312\rangle$	$\rightarrow 8$	51	$\langle 33311\rangle + \langle 33322\rangle$	(B3)
18	$\langle 11321\rangle + \langle 22312\rangle$	$\rightarrow 9$	52	$\langle 33231\rangle + \langle 33132\rangle$	$\rightarrow 46$
19	$\langle 13211\rangle + \langle 23122\rangle$	$\rightarrow 16$	53	$\langle 33131\rangle + \langle 33232\rangle$	$\rightarrow 51$
20	$\langle 13111\rangle + \langle 23222\rangle$		54	$\langle 32331\rangle + \langle 31332\rangle$	(B3)
21	$\langle 12311\rangle + \langle 21322\rangle$		55	$\langle 31331\rangle + \langle 32332\rangle$	(B3)
22	$\langle 11311\rangle + \langle 22322\rangle$		56	$\langle 33213\rangle + \langle 33123\rangle$	$\rightarrow 46$
23	$\langle 12231\rangle + \langle 21132\rangle$	$\rightarrow 8$	57	$\langle 33113\rangle + \langle 33223\rangle$	$\rightarrow 51$
24	$\langle 11231\rangle + \langle 22132\rangle$	$\rightarrow 9$	58	$\langle 32313\rangle + \langle 31323\rangle$	$\rightarrow 54$
25	$\langle 12131\rangle + \langle 21232\rangle$	$\rightarrow 21$	59	$\langle 31313\rangle + \langle 32323\rangle$	$\rightarrow 55$
26	$\langle 11131\rangle + \langle 22232\rangle$	$\rightarrow 22$	60	$\langle 32133\rangle + \langle 31233\rangle$	$\rightarrow 54$
27	$\langle 13331\rangle + \langle 23332\rangle$	(B3)	61	$\langle 31133\rangle + \langle 32233\rangle$	$\rightarrow 55$
28	$\langle 21113\rangle + \langle 12223\rangle$	$\rightarrow 10$	62	$\langle 33333\rangle$	(B3)
29	$\langle 22113\rangle + \langle 11223\rangle$	$\rightarrow 11$	63	$\langle 23111\rangle + \langle 13222\rangle$	(B3)
30	$\langle 21213\rangle + \langle 12123\rangle$	$\rightarrow 8$	64	$\langle 23211\rangle + \langle 13122\rangle$	$\rightarrow 15$
31	$\langle 22213\rangle + \langle 11123\rangle$	$\rightarrow 9$	65	$\langle 21311\rangle + \langle 12322\rangle$	$\rightarrow 10$
32	$\langle 23313\rangle + \langle 13323\rangle$	$\rightarrow 14$	66	$\langle 22311\rangle + \langle 11322\rangle$	$\rightarrow 11$
33	$\langle 12213\rangle + \langle 21123\rangle$	$\rightarrow 8$	67	$\langle 23121\rangle + \langle 13212\rangle$	$\rightarrow 15$
34	$\langle 11213\rangle + \langle 22123\rangle$	$\rightarrow 9$	68	$\langle 23221\rangle + \langle 13112\rangle$	$\rightarrow 16$

$$
\begin{aligned}
0 &= \Xi_{in}\Big[\chi^{(\mathrm{p4})}_{njk} - \Big[\chi^{(\mathrm{p43})}_{njklm} + \chi^{(\mathrm{p50})}_{njklm} + \chi^{(\mathrm{p55})}_{njklm}\Big]\hat{M}_l\hat{M}_m\Big] \\
&\quad \times \hat{M}_k, \\
0 &= \Xi_{in}\Big[\chi^{(\mathrm{p4})}_{njk} + \Big[\chi^{(\mathrm{p8})}_{njklm} + \chi^{(\mathrm{p22})}_{njklm} - \chi^{(\mathrm{p43})}_{njklm} \\
&\quad - \chi^{(\mathrm{p50})}_{njklm}\Big]\hat{M}_l\hat{M}_m\Big]\hat{M}_k, \\
0 &= \Xi_{in}\Big[\chi^{(\mathrm{p6})}_{njk} - \Big[\chi^{(\mathrm{p10})}_{njklm} + \chi^{(\mathrm{p21})}_{njklm} + \chi^{(\mathrm{p40})}_{njklm}\Big] \\
&\quad \times \hat{M}_l\hat{M}_m\Big]\hat{M}_k, \\
0 &= \Xi_{in}\Big[\chi^{(\mathrm{p7})}_{njk} - \Big[\chi^{(\mathrm{p11})}_{njklm} + \chi^{(\mathrm{p22})}_{njklm} + \chi^{(\mathrm{p41})}_{njklm}\Big] \\
&\quad \times \hat{M}_l\hat{M}_m\Big]\hat{M}_k, \qquad \text{(B3)}
\end{aligned}
$$

we may additionally set $\beta_{\#} = 0$ in Eq. (B2) for $\# = 5, 27, 40, 41, 46, 49, 50, 51, 54, 55, 62, 63$. Thus, there are only six linearly independent polar tensors of rank 3 and 12 linearly independent polar tensors of rank 5 that need to be considered in Eq. (B2), i.e., 18 tensors in total and 18 corresponding fitting parameters $\beta_{\#}$.

[1] A. Manchon, J. Železný, I. M. Miron, T. Jungwirth, J. Sinova, A. Thiaville, K. Garello, and P. Gambardella, Current-induced spin-orbit torques in ferromagnetic and antiferromagnetic systems, Rev. Mod. Phys. **91**, 035004 (2019).

[2] I. Galanakis, P. Mavropoulos, and P. H. Dederichs, Electronic structure and SlaterPauling behaviour in half-metallic Heusler alloys calculated from first principles, J. Phys. D **39**, 765 (2006).

[3] K. Elphick, W. Frost, M. Samiepour, T. Kubota, K. Takanashi, S. Hiroaki, S. Mitani, and A. Hirohata, Heusler alloys for spintronic devices: Review on recent development and future perspectives, Sci. Technol. Adv. Mater. **22**, 235 (2020).

[4] J. Ma, V. I. Hegde, K. Munira, Y. Xie, S. Keshavarz, D. T. Mildebrath, C. Wolverton, A. W. Ghosh, and W. H. Butler, Computational investigation of half-Heusler compounds for spintronics applications, Phys. Rev. B **95**, 024411 (2017).

[5] F. Casper, T. Graf, S. Chadov, B. Balke, and C. Felser, Half − Heusler compounds: Novel materials for energy and spintronic applications, Semicond. Sci. Technol. **27**, 063001 (2012).

[6] B. Kwon, Y. Sakuraba, H. Sukegawa, S. Li, G. Qu, T. Furubayashi, and K. Hono, Anisotropic magnetoresistance and current-perpendicular-to-plane giant magnetoresistance in epitaxial NiMnSb-based multilayers, J. Appl. Phys. **119**, 023902 (2016).

[7] Z. Wen, T. Kubota, T. Yamamoto, and K. Takanashi, Enhanced current-perpendicular-to-plane giant magnetoresistance effect in half-metallic NiMnSb based nanojunctions with multiple Ag spacers, Appl. Phys. Lett. **108**, 232406 (2016).

[8] G. Qu, P.-H. Cheng, Y. Du, Y. Sakuraba, S. Kasai, and K. Hono, Investigation of spin-dependent transports and microstructure in NiMnSb-based magnetoresistive devices, Appl. Phys. Lett. **111**, 222402 (2017).

[9] Z. Wen, T. Kubota, T. Yamamoto, and K. Takanashi, Fully epitaxial c1b-type NiMnSb half-Heusler alloy films for current-perpendicular-to-plane giant magnetoresistance devices with a Ag spacer, Sci. Rep. **5**, 18387 (2015).

[10] C. Liu, C. K. A. Mewes, M. Chshiev, T. Mewes, and W. H. Butler, Origin of low gilbert damping in half metals, Appl. Phys. Lett. **95**, 022509 (2009).

[11] C. Ciccarelli, L. Anderson, V. Tshitoyan, A. J. Ferguson, F. Gerhard, C. Gould, L. W. Molenkamp, J. Gayles, J. Zelezny, L. Smejkal, Z. Yuan, J. Sinova, F. Freimuth, and T. Jungwirth, Room-temperature spin orbit torque in NiMnSb, Nat. Phys. **12**, 855 (2016).

[12] J. elezn, Z. Fang, K. Olejnk, J. Patchett, F. Gerhard, C. Gould, L. W. Molenkamp, C. Gomez-Olivella, J. Zemen, T. Tich, T. Jungwirth, and C. Ciccarelli, Unidirectional magnetoresistance and spin-orbit torque in NiMnSb, arXiv:2102.12838 [cond-mat.mes-hall].

[13] N. Zhao, A. Sud, H. Sukegawa, S. Komori, K. Rogdakis, K. Yamanoi, J. Patchett, J. W. A. Robinson, C. Ciccarelli, and H. Kurebayashi, Growth, strain, and spin-orbit torques in epitaxial Ni-Mn-Sb films sputtered on GaAs, Phys. Rev. Mater. **5**, 014413 (2021).

[14] J. Železný, H. Gao, A. Manchon, F. Freimuth, Y. Mokrousov, J. Zemen, J. Mašek, J. Sinova, and T. Jungwirth, Spin-orbit torques in locally and globally noncentrosymmetric crystals: Antiferromagnets and ferromagnets, Phys. Rev. B **95**, 014403 (2017).

[15] K. Garello, I. M. Miron, C. O. Avci, F. Freimuth, Y. Mokrousov, S. Blügel, S. Auffret, O. Boulle, G. Gaudin, and P. Gambardella, Symmetry and magnitude of spin-orbit torques in ferromagnetic heterostructures, Nat. Nanotechnol. **8**, 587 (2013).

[16] F. Mahfouzi and N. Kioussis, First-principles study of the angular dependence of the spin-orbit torque in Pt/Co and Pd/Co bilayers, Phys. Rev. B **97**, 224426 (2018).

[17] J.-P. Hanke, F. Freimuth, B. Dupé, J. Sinova, M. Kläui, and Y. Mokrousov, Engineering the dynamics of topological spin textures by anisotropic spin-orbit torques, Phys. Rev. B **101**, 014428 (2020).

[18] K. D. Belashchenko, A. A. Kovalev, and M. van Schilfgaarde, First-principles calculation of spin-orbit torque in a Co/Pt bilayer, Phys. Rev. Mater. **3**, 011401(R) (2019).

[19] J. Krieft, J. Mendil, M. H. Aguirre, C. O. Avci, C. Klewe, K. Rott, J.-M. Schmalhorst, G. Reiss, P. Gambardella, and T. Kuschel, Co-sputtered PtMnSb thin films and PtMnSb/Pt bilayers for spin-orbit torque investigations, Phys. Status Solidi RRL **11**, 1600439 (2017).

[20] M. C. Kautzky and B. M. Clemens, Structure and magneto-optical properties of epitaxial PtMnSb(001) on W(001)/MgO(001), Appl. Phys. Lett. **66**, 1279 (1995).

[21] P. G. van Engen, K. H. J. Buschow, R. Jongebreur, and M. Erman, PtMnSb, a material with very high magneto-optical kerr effect, Appl. Phys. Lett. **42**, 202 (1983).

[22] V. N. Antonov, P. M. Oppeneer, A. N. Yaresko, A. Y. Perlov, and T. Kraft, Computationally based explanation of the peculiar magneto-optical properties of PtMnSb and related ternary compounds, Phys. Rev. B **56**, 13012 (1997).

[23] M. C. Kautzky, F. B. Mancoff, J.-F. Bobo, P. R. Johnson, R. L. White, and B. M. Clemens, Investigation of possible giant magnetoresistance limiting mechanisms in epitaxial PtMnSb thin films, J. Appl. Phys. **81**, 4026 (1997).

[24] Z. Wen, T. Kubota, and K. Takanashi, Optimization of half-HeuslerPtMnSb alloy films for spintronic device applications, J. Phys. D **51**, 435002 (2018).

[25] F. Freimuth, S. Blügel, and Y. Mokrousov, Spin-orbit torques in Co/Pt(111) and Mn/W(001) magnetic bilayers from first principles, Phys. Rev. B **90**, 174423 (2014).

[26] R. R. Birss, *Symmetry and Magnetism* (North-Holland, Amsterdam, 1964).

[27] J. P. Perdew, K. Burke, and M. Ernzerhof, Generalized Gradient Approximation Made Simple, Phys. Rev. Lett. **77**, 3865 (1996).

[28] See http://www.flapw.de.

[29] U. von Barth and L. Hedin, A local exchange-correlation potential for the spin polarized case. i, J. Phys. C **5**, 1629 (1972).

[30] C. Li, A. J. Freeman, H. J. F. Jansen, and C. L. Fu, Magnetic anisotropy in low-dimensional ferromagnetic systems: Fe monolayers on Ag(001), Au(001), and Pd(001) substrates, Phys. Rev. B **42**, 5433 (1990).

[31] G. Pizzi, V. Vitale, R. Arita, S. Blügel, F. Freimuth, G. Géranton, M. Gibertini, D. Gresch, C. Johnson, T. Koretsune *et al.*, Wannier90 as a community code: new features and applications, J. Phys.: Condens. Matter **32**, 165902 (2020).